Int. J. Heat Mass Transfer. Vol. 33, No. 10, pp. 2247–2264, 1990
Printed in Great Britain

0017–9310 90 $3.00 + 0.00
Pergamon Press plc

Calculation of turbulent buoyant plumes with a Reynolds stress and heat flux transport closure

M. R. MALIN
CHAM Limited, Bakery House, 40 High Street, Wimbledon, London SW19 5AU, U.K.

and

B. A. YOUNIS
Department of Civil Engineering, City University, London, U.K.

(*Received* 8 *August* 1989)

Abstract—A differential Reynolds stress and heat flux closure is adopted for modelling the turbulent transport of heat and momentum in vertical buoyant free plumes. Modelled transport equations are solved for the turbulent stresses and heat fluxes, the turbulence energy dissipation rate, and the mean-square temperature fluctuations. Closure at this level permits the turbulent transport processes to be treated more exactly than with Boussinesq-type two-equation models which are based on the notion of an effective viscosity and diffusivity. The solution of a transport equation for the thermal dissipation rate, which avoids the need to empirically prescribe the ratio of the thermal and mechanical time scales, is also investigated. The model is applied to the calculation of both self-similar plumes and forced plumes. The results are compared with existing experimental data and are found to be in reasonable agreement with the measured behaviour.

1. INTRODUCTION

TURBULENT plumes, such as those that occur in engineering practice exemplified by the flow from smoke stacks, cooling towers and submerged waste-disposal systems, are often buoyant: their mean-flow features and turbulence structure being strongly modified by the gravitational field. The prediction of such flows has in most cases utilized turbulence models based on the notions of isotropic eddy viscosity and constant turbulent Prandtl number, both assumptions unsupported by experiment. It is not surprising, therefore, that these models, while yielding acceptable results for simple non-buoyant shear flows, fail to reproduce the effects of buoyancy unless modified quite severely in some respect. One popular route for improving the performance of standard eddy-viscosity models for buoyancy has been to use them in conjunction with algebraic stress/flux models (ASM) that are capable of reproducing the observed anisotropy of the turbulence field wrought by buoyancy. Such models are derived by simplifying transport equations for the individual turbulent stresses and fluxes such that they reduce to algebraic expressions for these correlations. Successful predictions of turbulent plumes based on this approach have been reported by several workers [1–3].

Although ASMs have proved to be fairly successful at simulating turbulent plumes, the adoption of such a closure means that the transport of the turbulent stresses and heat fluxes is treated fairly simply, and as a consequence, such models have been found unsuitable [3, 4] for situations too far removed from equilibrium, as for example in strongly-stratified flows. For general elliptic flows, the ASM expressions are also rather complex and difficult to implement in numerical procedures, and so the advantages over full-transport models are lessened or even negated. The alternative and more direct approach to modelling the turbulence in buoyancy-affected shear flows is to obtain the unknown Reynolds stresses and heat fluxes from the solution of the original modelled differential transport equations [5–7]. Such a model now takes direct account of the transport and history effects on these individual stress and flux components, and thus is able to simulate the physical processes more realistically. This approach seems to be more generally applicable for modelling the more complex buoyant flows associated with engineering and environmental applications. While the ultimate objective is to have a model applicable to the calculation of such practical flows, the simple vertical buoyant plumes considered in this study provide an essential basic test of the modelling procedures.

The Reynolds-stress and heat-flux transport model of Launder *et al.* [5–7] has given reasonably good results for vertical jets and plumes [8, 9], although it has been found that the plane wall jet cannot be simulated accurately with the standard set of model coefficients [9]. This basic model which employs the simplest of the pressure–strain models suggested in ref. [5], also fails to predict correctly the development of swirling jets and curved flows that are independent of the coordinate system. Calculations with the more complex expression for the pressure–strain fared no better, and in fact proved even less satisfactory than

NOMENCLATURE

c's	empirical constants in the turbulence model
d	source dimension
f	wall-damping function
F_D	densimetric Froude number
g	gravitational acceleration
g_i	component i of the gravitation vector
G_{ij}	buoyancy production of $\overline{u_iu_j}$
G_{it}	production of $\overline{u_it'}$ due to buoyancy
j	exponent : 0, for plane flows ; 1, for axisymmetric flows
k	turbulent kinetic energy
P	static pressure
P_{ij}	stress production of $\overline{u_iu_j}$
$P_{it,1}$	production of $\overline{u_it'}$ due to mean-temperature gradients
$P_{it,2}$	production of $\overline{u_it'}$ due to mean-velocity gradients
P_t	production rate of $\overline{t'^2}$
R	time-scale ratio
T	mean temperature
ΔT	temperature excess
t'	fluctuating temperature
$\overline{t'^2}$	mean-square temperature fluctuations
$\overline{u^2}$	streamwise turbulent normal stress
$\overline{u_iu_j}$	Reynolds stresses
$\overline{u_it'}$	Reynolds heat fluxes
$\overline{ut'}$	streamwise turbulent heat flux
$\overline{uv}$	cross-stream turbulent shear stress
U	streamwise velocity in the x-direction
U_m	maximum value of U velocity
U_i	mean velocity in the x_i-direction
$\overline{v^2}$	cross-stream turbulent normal stress
$\overline{vt'}$	cross-stream turbulent heat flux
$\overline{w^2}$	transverse or circumferential turbulent normal stress
x_i	spatial coordinate in the i-direction
x	streamwise coordinate.
y	cross-stream coordinate

Greek symbols

β	coefficient of volumetric expansion
δ_{ij}	Kronecker delta
δ_u	velocity half-width
δ_t	temperature half-width
ε	dissipation rate of k
ε_t	dissipation rate of $\overline{t'^2}$
π_{ij}	pressure redistribution of $\overline{u_iu_j}$
π_{it}	pressure redistribution of $\overline{u_it'}$
ρ	fluid density
$\Delta\rho$	density defect
σ's	empirical diffusion coefficients in turbulence model.

Superscripts

$'$	fluctuating quantities
$\bar{}$	mean quantities.

Subscripts

i, j	spatial coordinates
m	maximum value
r	reference value at local ambient conditions
0	source condition
∞	ambient condition.

the simpler model. Significant improvements for all of these cases may be effected by adopting the choice of model coefficients recommended by Gibson and Younis [10–13]. Moreover, the ability of the model to predict the development of simple shear flows remains unaffected. It is unnecessary to repeat here in detail the basis for this new set of model constants, but it is useful to point out that the constants are adjusted to give relatively less weight to the mean-strain part of the pressure–strain correlation, and more to the turbulent part. Consequently, the mean-strain part is reduced from levels indicated by rapid distortion theory, and the turbulent part is adjusted to conform with the measured rates of return to isotropy. It is found that the use of these new constants gives very good results for the plane wall jet [14], which is in fact a limiting case for the vertical bounded wall plume.

The objective of the present work is to extend the closure model of Gibson and Younis [10–13] to buoyant flows and to assess the performance of the complete Reynolds-stress and heat-flux transport model for free turbulent jets and plumes. A further novelty of the present contribution is that the dissipation rate of temperature variance may be obtained from a solution of its modelled transport equation [15, 16] rather than from an empirically-prescribed time-scale ratio as in previous studies of turbulent buoyant plumes.

2. THE MATHEMATICAL MODEL

2.1. *Mean flow equations*

The time-averaged equations for steady high Reynolds-number incompressible buoyant flow are written in cartesian-tensor form, as follows:

$$(\rho U_i)_{,i} = 0 \tag{1}$$

$$(\rho U_jU_i)_{,j} = -P_{,i} - (\rho\overline{u_iu_j})_{,j} + (\rho - \rho_r)g_i \tag{2}$$

$$(\rho U_jT)_{,j} = -(\rho\overline{u_jt'})_{,j} \tag{3}$$

$$\rho = \rho_rT_r/T \tag{4}$$

wherein $\overline{u_iu_j}$ and $\overline{u_jt'}$ are, respectively, the unknown Reynolds stresses and heat fluxes.

2.2. *The turbulence model*

The numerical solution of the above set of mean-flow equations is achieved by introducing additional transport equations for $\overline{u_iu_j}$ and $\overline{u_jt'}$. These equations contain higher-order correlations which must be approximated by model assumptions in order to close the system of equations. These higher-order correlations represent the processes of diffusive transport, viscous dissipation, and fluctuating pressure–velocity and pressure–temperature interactions.

The model assumptions adopted in this study have appeared in detail elsewhere in the literature [5–7, 10–13, 15, 16] and so only the main features are provided here. In summary, the present Reynolds stress and heat flux closure makes use of the linear return-to-isotropy approximation and the isotropization-of-production (IP) model for the pressure–strain terms, similar models for the pressure–temperature-gradient correlations, simple gradient-diffusion models for the diffusive transport, and the local isotropy assumption for viscous dissipation. The gradient-diffusion and local-isotropy assumptions are appropriate for the flows considered here, but it is understood that for more complex buoyant flows, the direct effect of buoyancy on these processes may have to be included, as done, for example, by Zeman and Lumley [17] for the diffusive transport.

The complete turbulence closure model is now outlined in the following sections.

2.2.1. *Reynolds stresses.* The Reynolds stresses are obtained from the following modelled transport equation:

$$(\rho U_k\overline{u_iu_j})_{,k} = c_s\left(\rho\overline{u_ku_l}\frac{k}{\varepsilon}(\overline{u_iu_j})_{,l}\right)_{,k} + \rho(P_{ij}+G_{ij}+\pi_{ij}-\tfrac{2}{3}\delta_{ij}\varepsilon) \quad (5)$$

wherein c_s is an empirical constant which is assigned a value of 0.22 [10–13]. The five terms appearing on the right-hand side of equation (5) denote respectively: diffusive transport; stress production due to mean shear and buoyancy; redistributive action of the pressure–strain correlations; and direct dissipation by viscous action. The turbulent stress diffusion process has been approximated by the gradient-diffusion model of Daly and Harlow [18], while local isotropy has been assumed for the dissipative correlations. Consequently, the dissipation term is zero for shear stresses, and for the normal stresses the same amount of energy is dissipated in each component of the turbulent kinetic energy.

The production terms P_{ij} and G_{ij} need no approximation and are defined by

$$P_{ij} = -(\overline{u_iu_k}U_{j,k}+\overline{u_ju_k}U_{i,k}) \quad (6)$$

$$G_{ij} = -\beta(g_i\overline{u_jt'}+g_j\overline{u_it'}) \quad (7)$$

wherein the volumetric coefficient of expansion is defined by $\beta = -(\partial\rho/\partial T)_p/\rho$.

The 'pressure–strain' term π_{ij} acts to redistribute energy among the various components and to reduce shear stresses. The term is modelled as the sum of three contributions

$$\pi_{ij} = \pi_{ij1}+\pi_{ij2}+\pi_{ij3} \quad (8)$$

the separate elements being associated respectively with purely turbulence interactions, interactions between mean strain and fluctuating velocities, and buoyancy forces. These three contributions are modelled as follows:

$$\pi_{ij1} = -c_1\frac{\varepsilon}{k}(\overline{u_iu_j}-\tfrac{2}{3}\delta_{ij}k) \quad (9)$$

$$\pi_{ij2} = -c_2(P_{ij}-\tfrac{1}{3}\delta_{ij}P_{kk}) \quad (10)$$

$$\pi_{ij3} = -c_3(G_{ij}-\tfrac{1}{3}\delta_{ij}G_{kk}) \quad (11)$$

where $(c_1, c_2, c_3) = (3.0, 0.3, 0.3)$ as recommended by Gibson and Younis [10–13]. Rotta's [19] linear return-to-isotropy model has been adopted for π_{ij1}, while the IP models of Launder *et al.* [5–7] have been used for π_{ij2} and π_{ij3}.

2.2.2. *Turbulent heat fluxes.* The turbulent heat fluxes are obtained from the following modelled transport equation:

$$(\rho U_k\overline{u_it'})_{,k} = c_t\left(\rho\frac{k}{\varepsilon}\overline{u_ku_l}(\overline{u_it'})_{,l}\right)_{,k} + \rho(P_{it,1}+P_{it,2}+G_{it}+\pi_{it}) \quad (12)$$

where the constant c_t is taken equal to 0.15 [8, 9]. The five terms appearing on the right-hand side of equation (12) denote respectively: diffusive transport; production due to mean-temperature gradients; production due to mean-velocity gradients; production due to buoyancy; and the action of the pressure–temperature-gradient correlations. The viscous destruction term has been neglected by invoking the local isotropy assumption for high turbulent Reynolds numbers; and a gradient-type model has been adopted for the turbulent-heat-flux diffusion process.

The production terms which require no approximation are defined by

$$P_{it,1} = -\overline{u_ku_l}T_{,k} \quad (13)$$

$$P_{it,2} = -\overline{u_kt'}U_{i,k} \quad (14)$$

$$G_{it} = -\beta g_i\overline{t'^2} \quad (15)$$

where $\overline{t'^2}$ is the mean square of the temperature fluctuations.

The pressure–temperature-gradient correlation π_{it} is the counterpart of the pressure–strain term in the $\overline{u_iu_j}$ equation and generally, it acts to reduce $\overline{u_it'}$. It is modelled as the sum of three terms

$$\pi_{it} = \pi_{it1}+\pi_{it2}+\pi_{it3} \quad (16)$$

the separate components being associated respectively

with purely turbulence interactions, interactions between mean strain and fluctuating quantities, and buoyancy forces. These three contributions are modelled as follows:

$$\pi_{it1} = -c_{1t}\frac{\varepsilon}{k}\overline{u_i t'} \tag{17}$$

$$\pi_{it2} = -c_{2t}P_{it,2} \tag{18}$$

$$\pi_{it3} = -c_{3t}G_{it} \tag{19}$$

wherein $(c_{1t}, c_{2t}, c_{3t}) = (2.85, 0.55, 0.55)$. Following Launder [6], these empirical coefficients have been estimated by reference to homogeneous shear-flow data on the streamwise and cross-stream heat fluxes. The model for π_{it1} is that of Monin [20] which can be seen to be a counterpart of Rotta's 'return-to-isotropy' approximation (9) for the pressure–strain term π_{ij1}. The models adopted for π_{it2} and π_{it3} are those proposed by Launder [6] in analogy to the pressure–strain models (10) and (11).

2.2.3. *Turbulence energy dissipation rate.* The turbulence energy dissipation rate ε is computed from the following modelled transport equation:

$$(\rho U_k\varepsilon)_{,k} = c_\varepsilon\left(\rho\frac{k}{\varepsilon}\overline{u_k u_l}\varepsilon_{,l}\right)_{,k} + \rho\frac{\varepsilon}{k}\tfrac{1}{2}(c_{1\varepsilon}P_{kk} + c_{3\varepsilon}G_{kk} - 2c_{2\varepsilon}\varepsilon) \tag{20}$$

where $(c_\varepsilon, c_{1\varepsilon}, c_{2\varepsilon}) = (0.15, 1.4, 1.8)$ as recommended by Gibson and Younis [10–13]. The first term on the right-hand side of this equation represents diffusive transport by the turbulent motion. The remaining terms model the difference between the production and destruction terms appearing in the exact transport equation for the dissipation rate.

Buoyancy effects enter in equation (20) through the buoyancy production term G_{kk}, and the value of the empirical constant $c_{3\varepsilon}$ has been given a value of 0.98 so as to yield satisfactory results for the free line plume. This value agrees closely with that used in previous applications of stress transport closures [8, 9, 21], and contrasts with the experience of algebraic stress models [2] which return good results with $c_{3\varepsilon} = c_{1\varepsilon}$. This very different behaviour of the algebraic and differential stress closures has been commented upon by other workers [8, 21]. Although a single value for $c_{3\varepsilon}$ and $c_{1\varepsilon}$ is desirable, there is, however, no reason to expect that the modelled sources of ε associated with mean shear and buoyancy should appear in the ε-equation with the same coefficient. In fact, it is widely known that a value of $c_{3\varepsilon}$ close to zero is appropriate for horizontal surface jets with stable stratification [4].

2.2.4. *Temperature fluctuations.* The temperature fluctuations $\overline{t'^2}$ are computed from the following modelled transport equation:

$$(\rho U_k\overline{t'^2})_{,k} = c_\theta\left(\rho\frac{k}{\varepsilon}\overline{u_k u_l}\overline{t'^2}_{,l}\right)_{,k} + \rho(P_t - 2\varepsilon_t) \tag{21}$$

where the constant c_θ is taken as 0.11 [8, 9]. This equation is required for closure in buoyant flows because the temperature variance appears in the buoyancy production term (15) of the $\overline{u_i t'}$ equation. The three terms appearing on the right-hand side of equation (21) represent respectively: diffusive transport; production due to mean-temperature gradients; and dissipation due to molecular action in the fine-scale motions.

The production rate of $\overline{t'^2}$ which requires no approximation is given by

$$P_t = -2\overline{u_j t'}T_{,j} \tag{22}$$

and the dissipation rate ε_t of the temperature fluctuations is determined either from its own modelled transport equation [15, 16], or by assuming a constant ratio of the thermal and mechanical time scales

$$\varepsilon_t = \frac{\overline{t'^2}\varepsilon}{2kR} \tag{23}$$

where R is the time scale ratio which is assigned a value of 0.56 [3, 9], rather than the commonly-used value of 0.8 [2, 4, 6, 7]. This assignment agrees closely with that employed by other workers [8] for similar flows, and follows from the original work of Spalding [22] who found that this value predicts correctly the level of concentration fluctuations in non-buoyant jets. The value of 0.8 is supported by data on stably-stratified free shear flows [23].

2.2.5. *Dissipation rate of temperature fluctuations.* There is enough evidence [23] to show that R is not sufficiently constant for equation (23) to serve as a general method of finding ε_t, and so several workers have advocated the use of a modelled transport equation for determining this quantity. Strictly speaking, the original transport models of Launder, Lumley and co-workers [17, 24, 25] are not applicable to flows with mean strain, and so in subsequent work Jones and Musonge [15, 16] extended these formulations by introducing a term involving the production rate of turbulent kinetic energy. The resulting transport model was then applied to calculate successfully a number of self-similar turbulent shear flows. This model of Jones and Musonge [15, 16] is used in the present study, and it takes the form

$$(\rho U_k\varepsilon_t)_{,k} = c_{\varepsilon t}\left(\rho\frac{k}{\varepsilon}\overline{u_k u_l}\varepsilon_{t,l}\right)_{,k} + \rho\left(c_{\varepsilon t3}\frac{\varepsilon_t}{\overline{t'^2}}P_t + c_{\varepsilon t4}P_{kk}\frac{\varepsilon_t}{2k} - c_{\varepsilon t1}\frac{\varepsilon_t^2}{\overline{t'^2}} - c_{\varepsilon t2}\frac{\varepsilon\varepsilon_t}{k}\right) \tag{24}$$

where $(c_{\varepsilon t}, c_{\varepsilon t1}, c_{\varepsilon t2}, c_{\varepsilon t3}, c_{\varepsilon t4}) = (0.09, 2.0, 0.8, 0.5, 1.4)$. The majority of these constants are taken from Jones

and Musonge [15, 16], although $c_{\varepsilon t2}$ and $c_{\varepsilon t4}$ have been adjusted slightly to conform with the values of $c_{1\varepsilon}$ and $c_{2\varepsilon}$ recommended by Gibson and Younis [10–13]. The five terms appearing on the right-hand side of equation (24) represent respectively: diffusive transport; production due to mean-temperature gradients; production due to mean shear; dissipation dependent on the thermal time scale; and dissipation dependent on the mechanical time scale. There is no direct buoyancy influence on ε_t, as the exact equation for this quantity does not involve any buoyancy terms.

2.3. *Boundary conditions*

For all the cases considered, the flow is symmetrical about the flow axis, and a zero-flux boundary condition is employed along the symmetry plane for all variables excepting the cross-stream shear stress $\overline{uv}$ and heat flux $\overline{vt'}$, which are both set to zero. At free-stream boundaries, a fixed-pressure condition is applied, and the streamwise velocities and temperatures are set equal to their ambient values, and zero values are prescribed for all turbulent quantities. The calculations start from the inlet plane which is located at the source of the plume or jet. At this location the distribution of all dependent variables must be specified before the calculation can start. For self-similar jets and plumes, the calculations are started with arbitrary inlet profiles, which is permissible because only the similarity solution is of interest in the present work. The inlet values employed for non-similar flows are given in Section 4.

3. SOLUTION OF THE EQUATIONS

The mean flow and turbulence model equations are parabolized in the main flow direction and solved numerically with the parabolic finite-volume procedure embodied in the PHOENICS computer program [26]. The solution is obtained as a marching integration in the x-direction, starting from prescribed values of all dependent variables at the source. Typically, the calculations utilize 40–50 cross-stream grid cells and a forward step size ranging between 2 and 5% of the local width of the shear layer.

The complete stress–flux transport model was introduced by utilizing the facilities provided by PHOENICS for the attachment of user-generated coding sequences. The most important features of this implementation were to stagger the location of the shear stress and heat flux relative to the mean-field nodes, to eliminate turbulent diffusive transport in the mean-field equations, and to introduce stress and heat-flux terms as sources into these equations.

It should be mentioned that the parabolic approximation brings with it the neglect of streamwise derivatives involving the vertical turbulent heat flux, namely $-\partial/\partial x(\overline{\rho ut'})$ in the mean-temperature equation, and $-2\overline{\rho ut'}\,\partial T/\partial x$ in the source of temperature fluctuations. Other workers [1, 8] have argued for the inclusion of these terms on the ground that they give, respectively, non-negligible contributions to the total heat flux and the production of temperature fluctuations. Nevertheless, previous calculations with these approximations have yielded sufficiently accurate predictions of plume flows [2, 3, 9].

4. RESULTS AND DISCUSSION

The model implementation was validated against a number of well-documented non-buoyant turbulent shear flows including the flat plate boundary layer, the plane and axisymmetric free jet and the plane wall jet. The results for the free jets are presented here in view of their importance as limiting cases for the calculation of free buoyant plumes.

It is the purpose of this section to show how the model is capable of simulating self-similar free jets and plumes, and also the more general case of a forced plume. For each case, a set of experimental data is selected as a basis of comparison, and the closure model is then applied so as to simulate these data. Similarity and scaling laws [3, 30, 31] are used to present the results in dimensionless form. These laws lead to certain expectations on the behaviour of turbulent jets and plumes, and are therefore useful for assessing the reliability of both prediction and experiment. The concept of similarity also allows data obtained in different experiments to be used together for model evaluation purposes, with the proviso, of course, that the measurements evidence the expected similarity behaviour.

4.1. *Self-similar turbulent jets*

In this section, the flows considered are heated axisymmetric (round) and plane jets exhausting into stagnant surroundings from a source of momentum with negligible buoyancy. The computed and measured similarity profiles of both mean-flow and turbulent quantities are shown in Figs. 1–4. Figures 1 and 2 present results for the plane jet, while Figs. 3 and 4 show results for the round jet. The figures include predictions made with a constant and variable time-scale ratio, the latter being determined via the solution of the transport equation for the thermal dissipation rate.

4.1.1. *Plane jet.* The calculated spreading rate $\mathrm{d}\delta_u/\mathrm{d}x = 0.1$ agrees fairly well with the range of experimental values reported by Rodi [29], i.e. $\mathrm{d}\delta_u/\mathrm{d}x = 0.1$–$0.11$. The thermal spreading rate $\mathrm{d}\delta_t/\mathrm{d}x$ is predicted at 0.13, which is somewhat lower than the experimental value of 0.14 recommended by Chen and Rodi [30], but in excellent agreement with the value of 0.128 recommended in the more recent review of Gouldin *et al.* [31].

Figure 1 reveals that the calculated mean velocity and shear stress profiles show good agreement with the plane-jet data [27], but as noted in earlier studies [13], the normal stress profiles are less satisfactorily predicted. However, there are considerable differences between the two sets of data [27, 28] for the normal

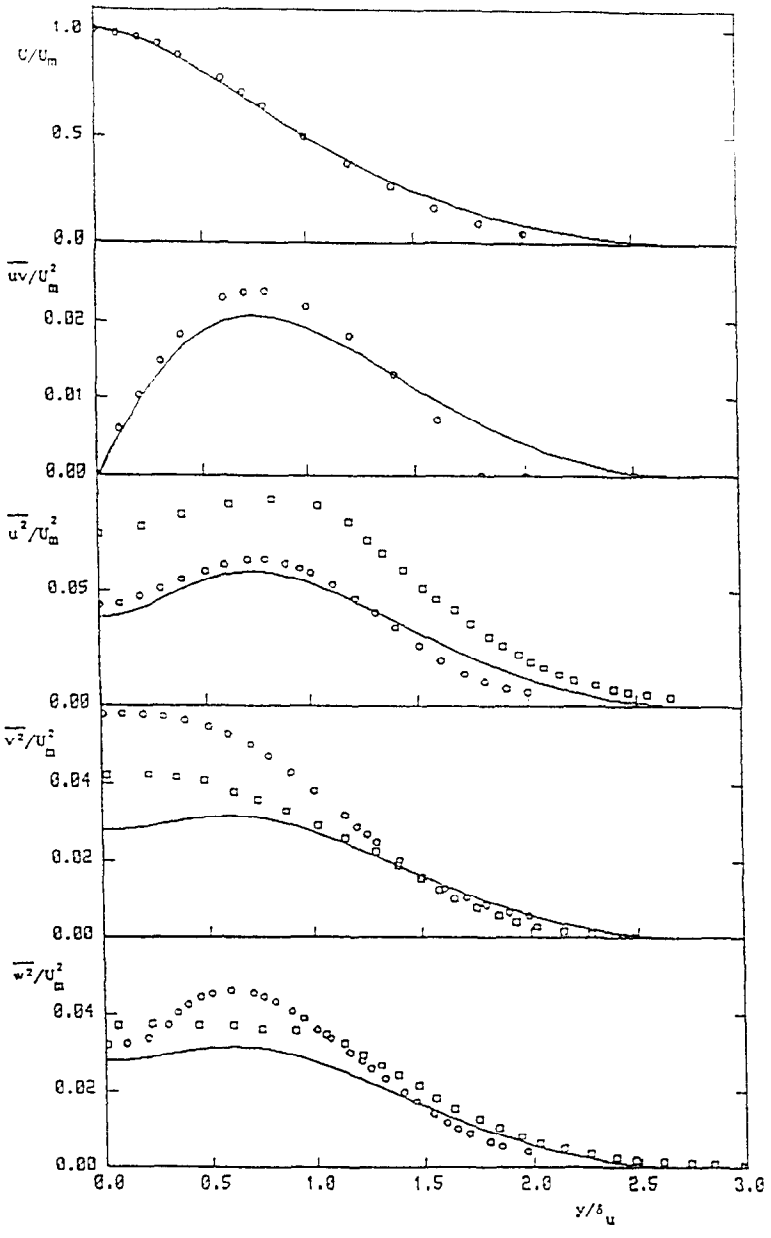

FIG. 1. Plane free jet: similarity profiles of mean velocity and Reynolds stresses. Data of: Bradbury [27], ○; Gutmark and Wygnanski [28], □. Predictions, ———.

stresses. The distribution of the mean temperature in Fig. 2 shows close agreement with the measurements [32]. The predicted profile shapes for each of the heat-flux components agree reasonably well with the data [33], but their magnitudes are overestimated. The figure shows, however, that the measured lateral heat fluxes are not satisfactory because they are appreciably below the values required to close the mean temperature equation. This appears to be a common difficulty with measurements of the heat flux in jets and plumes, and the problem has been discussed in some detail by List [35].

The distribution of the temperature fluctuations produced by each closure model agrees fairly well with the data [34], except perhaps in the highly intermittent outer region. The predictions obtained with the constant time-scale ratio are marginally better than those obtained via the solution of an equation for the thermal dissipation rate. From Fig. 2, it can also be seen that the predicted time-scale ratio varies across the flow, increasing gradually towards the free stream with an average value of about 0.5 in the bulk of the flow. This increase in R is in qualitative agreement with the experimental behaviour reported by Antonia [36].

4.1.2. *Round jet.* The predicted spreading rate $d\delta_u/dx = 0.103$, representing an increase of 20% over the value of 0.086 supported by experiments [29]. This

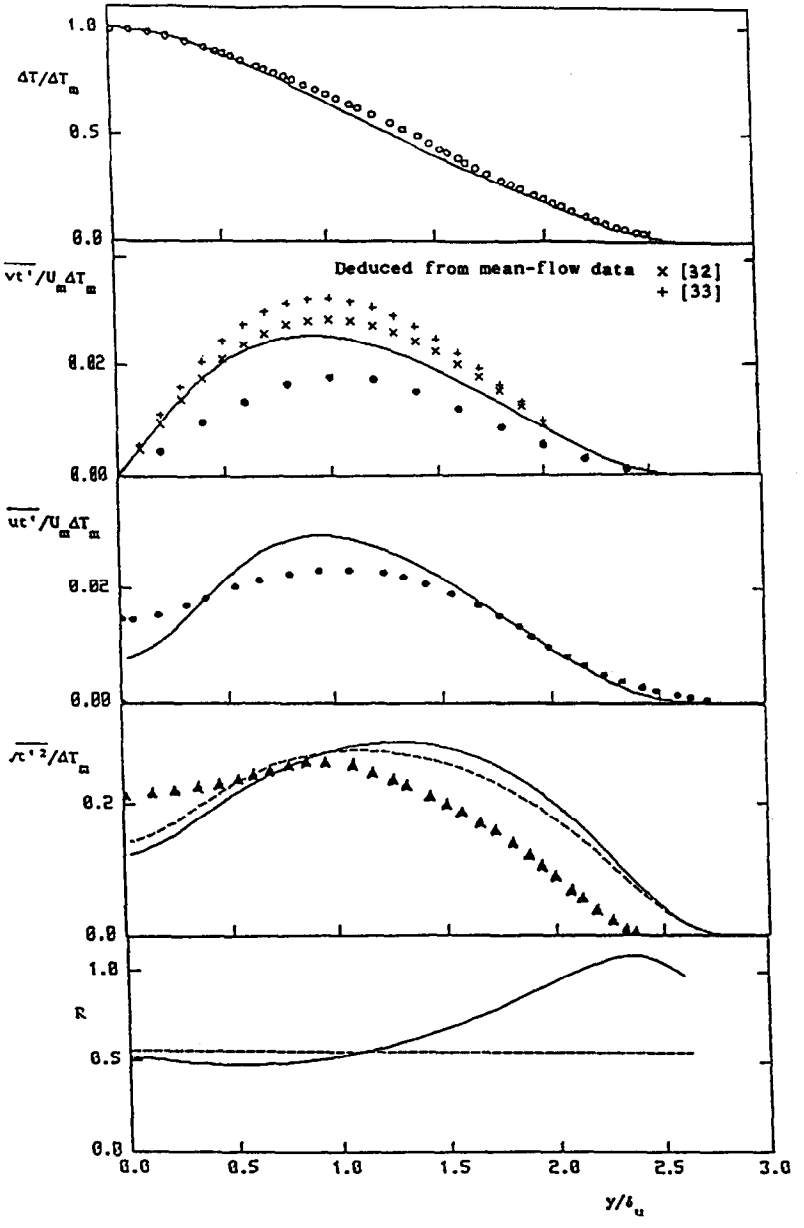

FIG. 2. Plane free jet: similarity profiles of mean temperature, turbulent heat fluxes, temperature fluctuations and time-scale ratio. Data of: Van der Hegge Zijnen [32], ○; Ramaprian and Chandrasekhara [33], ●; Bashir and Uberoi [34], ▲. Predictions, ———. Predictions ($R = 0.56$), — — —.

result represents a significant improvement over the values of 0.121 and 0.14 obtained with the two pressure–strain models proposed by Launder *et al.* [5]. The problem of predicting the spreading rates of plane and round jets with the same model is well known, and the anomaly is usually attributed to deficiencies in the modelled mechanical dissipation-rate equation (20). The thermal growth rate $d\delta_t/dx$ is predicted at 0.138, which is 25% higher than the value of 0.11 recommended by Chen and Rodi [30]. This discrepancy is due mainly to the inability of the model to obtain the correct velocity spreading rate.

Figure 3 shows that the calculated profile of mean velocity is in excellent agreement with the measured profile [29]. The predictions for the radial shear stress overestimate the measurements [29], which is consistent with the overprediction of the rate of spread. The agreement between the measured and calculated turbulent normal stresses is somewhat unsatisfactory, in that the Reynolds stress model underpredicts the measured values [29] in the core of the jet.

Turning to the thermal profiles shown in Fig. 4, it can be seen that the mean temperature profile is predicted satisfactorily, but the turbulent heat flux

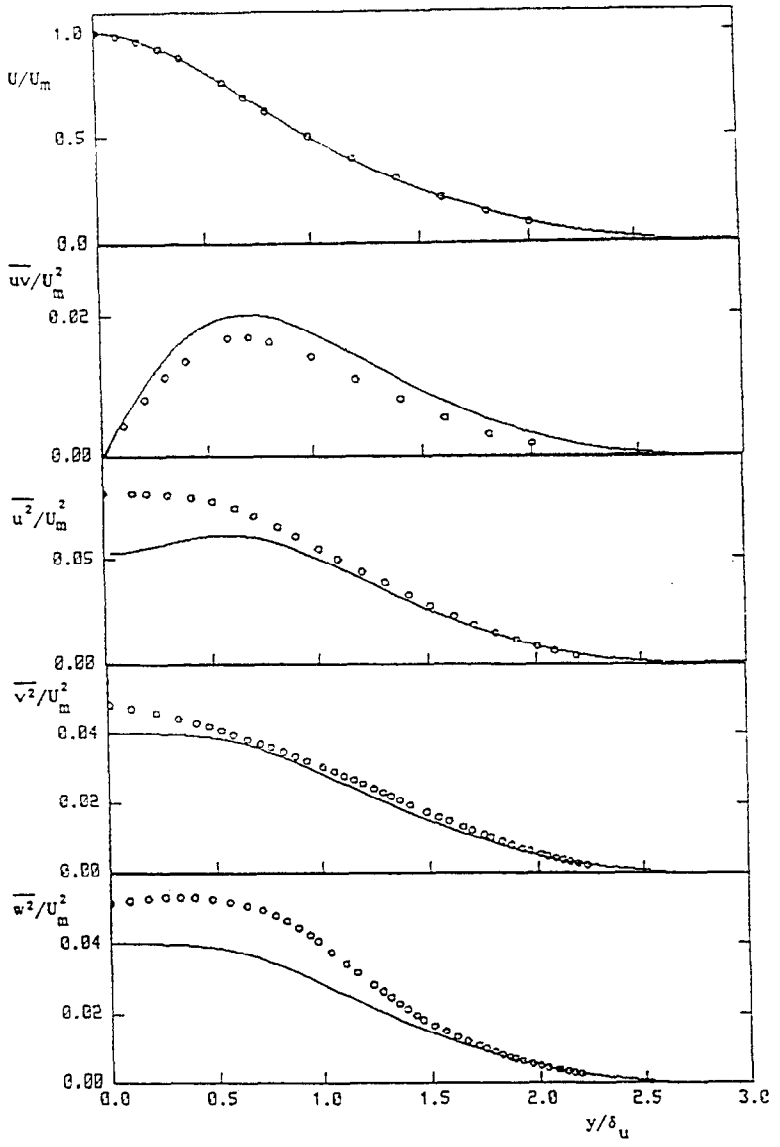

FIG. 3. Round free jet: similarity profiles of mean velocity and Reynolds stresses. Data of Rodi [29], O. Predictions, ———.

levels predicted by the model are largely in error. However, the experimental [37] radial heat fluxes correspond to a measuring station of $x/d = 15$, and therefore, they are not strictly similarity profiles because the turbulence becomes self-similar further downstream. Consequently, the measured heat fluxes are probably too low to be representative of a self-similar jet. In fact, the figure shows that the predicted distribution of $\overline{vt'}$ is much closer to the distribution determined from the mean velocity and mean temperature measurements [30]. The measured [38] axial heat flux levels are actually for a round jet in a co-flowing stream, and they are almost certainly too high for a jet in stagnant surroundings. For example, the turbulence levels reported by Antonia *et al.* [38] for other quantities are almost twice those reported by other experimenters for jets issuing into stagnant surroundings. For self-similar round jets, similarly profiles of $\overline{ut'}$ and $\overline{vt'}$ are not available.

Figure 4 also shows reasonable agreement between the predicted and measured [39] temperature fluctuations, with the constant time-scale closure yielding somewhat better predictions over the outer part of the flow. The computed variation of the time-scale ratio shown in Fig. 4 is broadly similar to that obtained for the plane jet, showing an average value of about 0.5 in the core of the jet.

4.2. *Self-similar turbulent plumes*

Turning now to buoyant flows, the cases considered are vertical turbulent plane and round plumes generated from a source of buoyancy with negligible

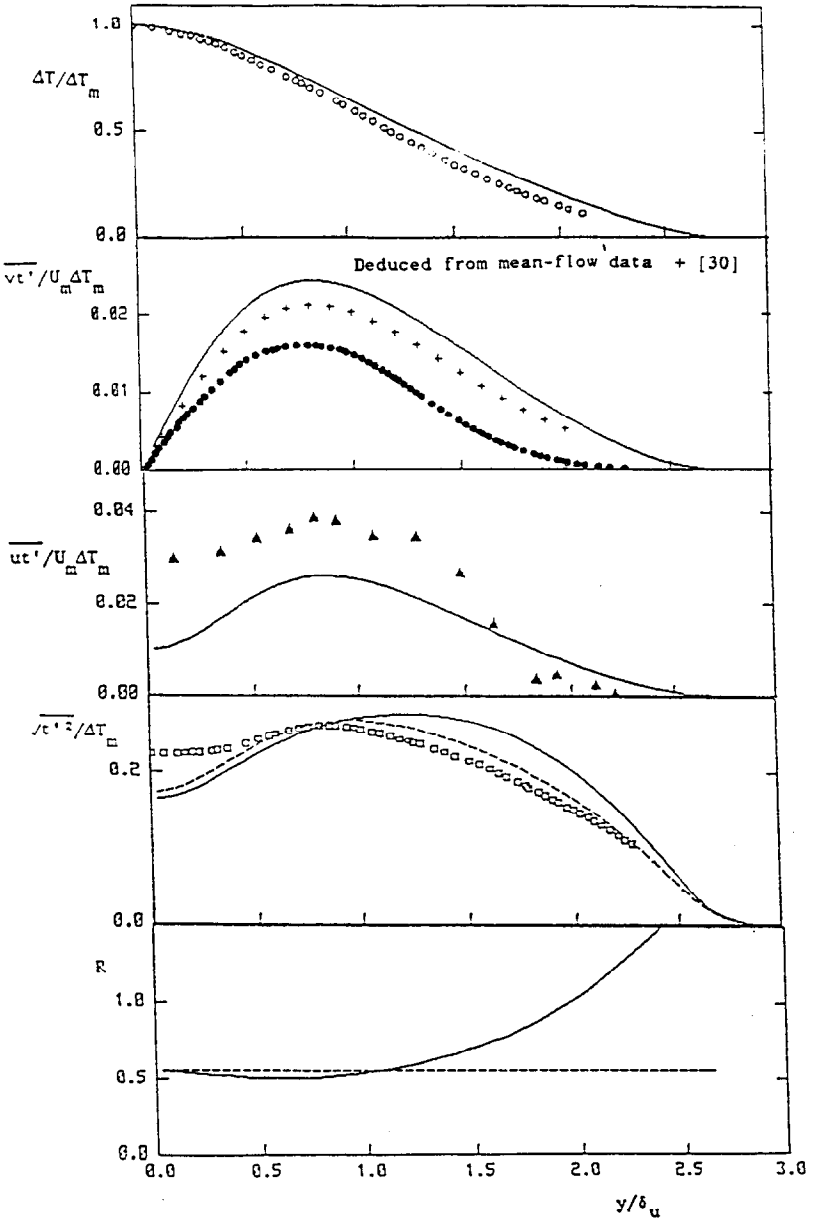

FIG. 4. Round free jet: similarity profiles of mean temperature, turbulent heat fluxes, temperature fluctuations and time-scale ratio. Data of: Chen and Rodi [30], ○; Chevray and Tutu [37], ●; Antonia *et al.* [38], ▲; Becker *et al.* [39], □. Predictions, ———. Predictions ($R = 0.56$), — — —.

momentum. Comparisons of the calculated and measured similarity profiles of both mean-flow and turbulent quantities are given in Figs. 5–8. Calculated results are shown for both constant and variable time-scale ratios. The results for the plane plume are displayed in Figs. 5 and 6, while Figs. 7 and 8 present results for the round plume.

4.2.1. *Plane plume.* Calculations of plane plumes with $c_{3\varepsilon} = c_{1\varepsilon}$ (see equation (20)) proved unsatisfactory as the computed spreading rates of $d\delta_u/dx = 0.081$ and $d\delta_t/dx = 0.089$ were fully 20% lower than those of experiments [33]. Here, it is noted that Haroutunian and Launder [8] reported similar discrepancies, even when terms involving streamwise gradients (neglected in this work) were included. Liauw [21] obtained satisfactory predictions by taking $c_{3\varepsilon}$ to be unity, and this is confirmed here because the measured spreading rate of 0.104 is reproduced with $c_{3\varepsilon} = 0.98$ (70% of its original value). The predicted value of $d\delta_t/dx$ is 0.111, which is in excellent agreement with the experimental value [33] of 0.11. The use of a constant time-scale ratio of 0.56 yields the almost identical spreading rates of $d\delta_u/dx = 0.105$ and $d\delta_t/dx = 0.113$.

The cross-stream profiles of mean velocity and turbulent stresses are compared with experiment [33] in

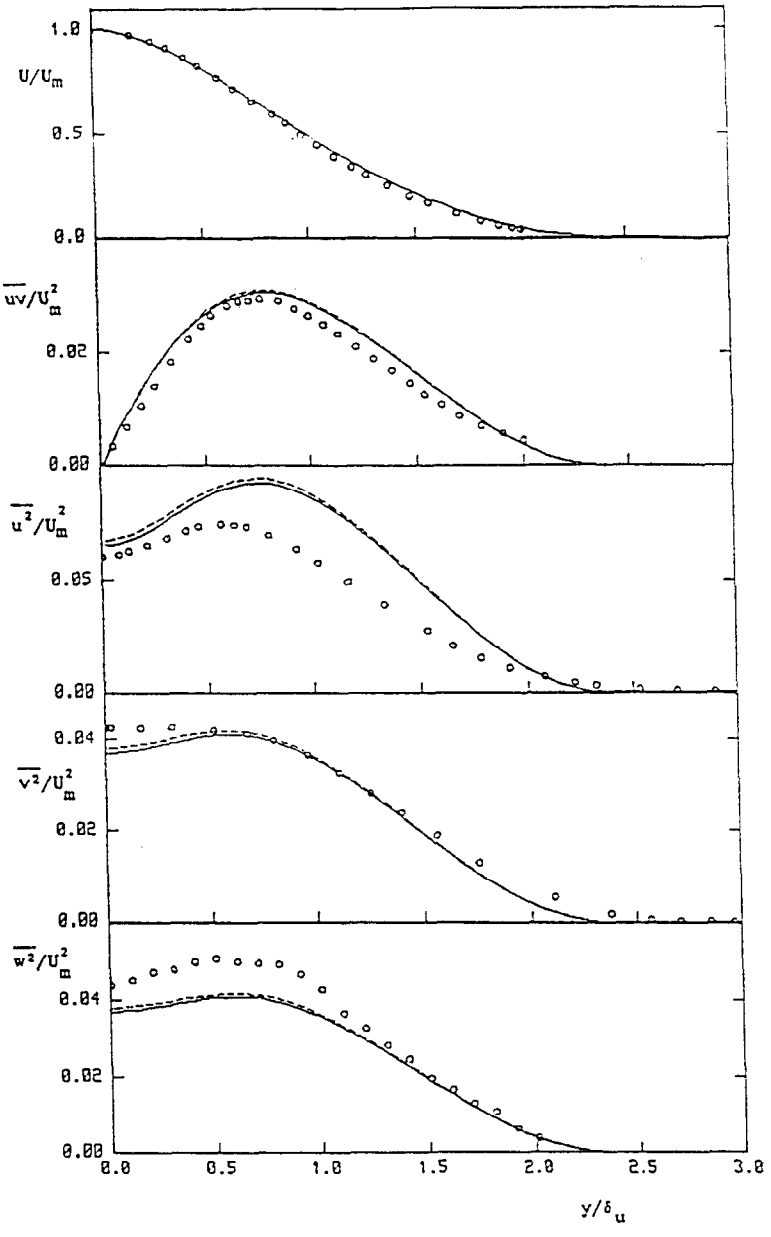

FIG. 5. Plane free plume: similarity profiles of mean velocity and Reynolds stresses. Data of Ramaprian and Chandrasekhara [33], ○. Predictions, ———. Predictions ($R = 0.56$), — — —.

Fig. 5. It can be seen that the differences between the variable and constant time-scale-ratio computations are small. The predicted lateral variations of the mean velocity and shear stress show good agreement with the data. The normal stresses are also reasonably well predicted, though the data on $\overline{u^2}$ suggest somewhat lower turbulence levels. It should be noted that $\overline{w^2}$ has been inferred from the data on $\overline{v^2}$ and $\overline{u^2}$. A comparison between the results for the plume and non-buoyant jet reveals that there is a general increase in the relative turbulence levels due to the influence of buoyancy. This trend is in agreement with the experimental findings.

Turning to the thermal results, Fig. 6 reveals that the agreement of the mean temperature profile is good, and it is noted here that the predictions are superior to those obtained from calculations with the old set of model coefficients proposed by Gibson and Launder [7], for which $d\delta_u/dx = 0.104$ and $d\delta_t/dx = 0.119$. From the same figure, it can be seen that the model predictions for the levels of the turbulent heat fluxes are much higher than those measured. The predicted magnitudes of $\overline{vt'}$ are considerably higher than those obtained by direct measurement [33], but as the figure shows, the data do not close the mean temperature equation. In fact, the predictions show close agreement with the levels of $\overline{vt'}$ deduced from the mean-flow measurements. The model indicates that the overall

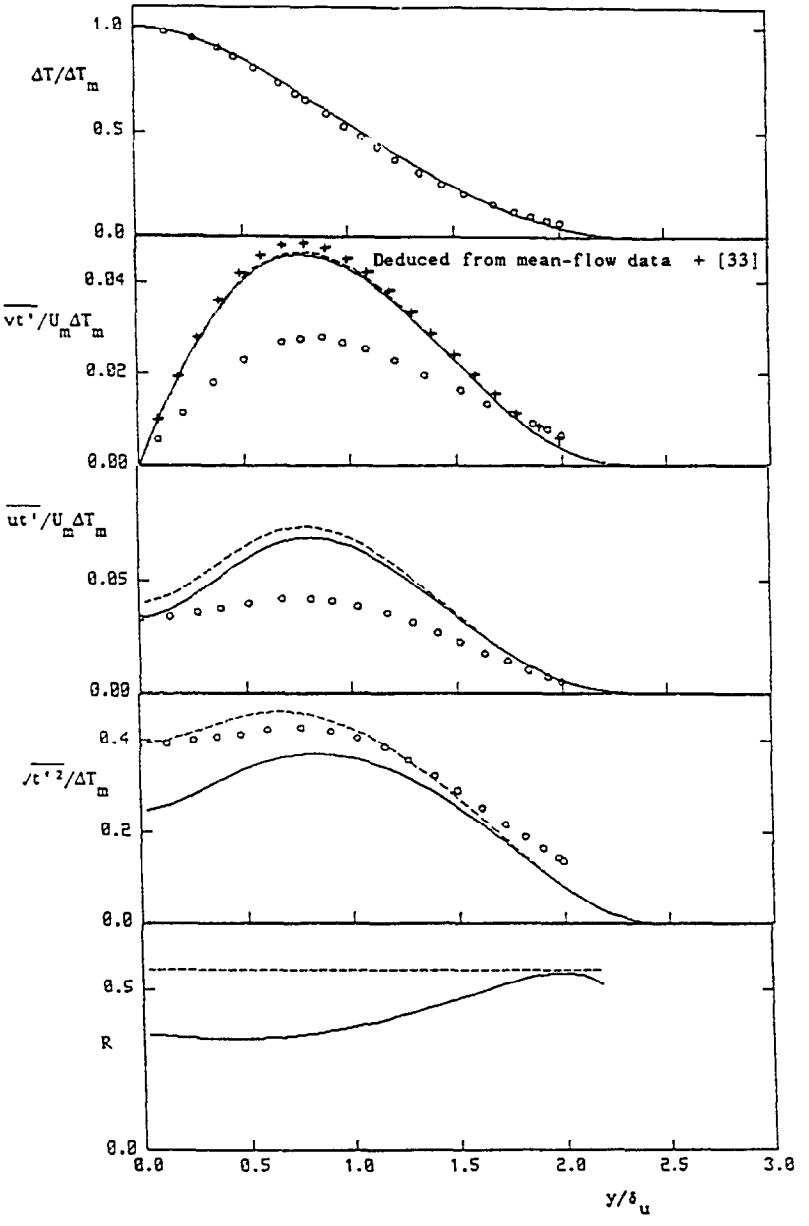

FIG. 6. Plane free plume: similarity profiles of mean temperature, turbulent heat fluxes, temperature fluctuations and time-scale ratio. Data of Ramaprian and Chandrasekhara [33], ○. Predictions, ———. Predictions ($R = 0.56$), — — —.

contribution $\overline{ut'}$ to the total vertical heat flux is about 10%, which is close to the experimental [33] range of 10–12%. Of course, the present calculations neglect the presence of this correlation in the mean temperature equation. Comparison of Fig. 6 with Fig. 2 reveals that the heat-flux profiles for the jet and plume are similar in shape, but the influence of buoyancy is to increase the relative turbulence levels considerably.

Attention is now turned to the predicted and measured temperature-fluctuation profiles shown in Fig. 6. The computations with a time-scale ratio of 0.56 produce intensities that are in good agreement with the data [33], and so the model predicts that the relative intensity is much higher in the plume than in the jet. This trend is in agreement with the experimental findings, as may be seen by comparing Fig. 6 with Fig. 2. On the other hand, the predictions of the temperature-fluctuation intensities obtained from the ε_t transport equation are about 35% too low in the core of the plume. This result follows from a decrease in the average value of R to about 0.36 (see Fig. 6), which may be explained by an increase in the thermal dissipation rate due to unstable stratification. The remainder of the thermal predictions, however, show very little sensitivity to this change in R, except that there is a noticeable reduction in $\overline{ut'}$ because of the

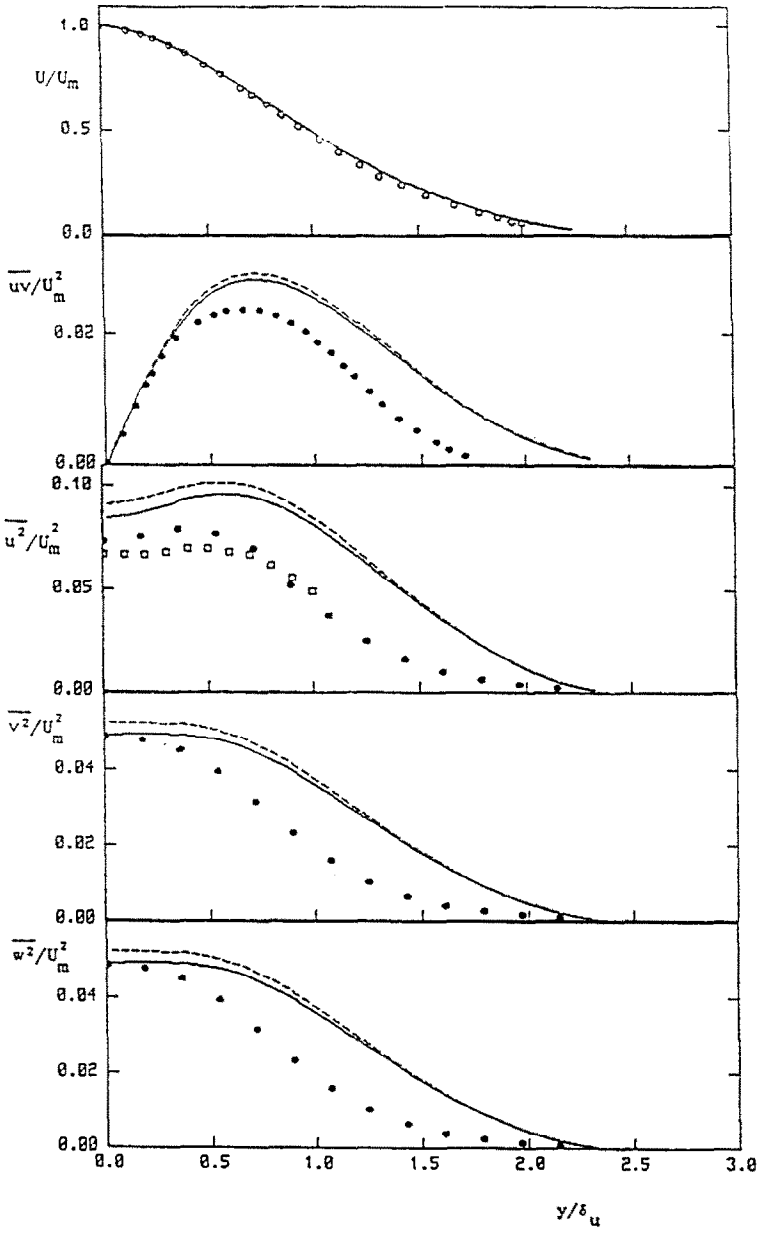

FIG. 7. Round free plume: similarity profiles of mean velocity and Reynolds stresses. Data of: George *et al.* [40], ○, □; Beuther *et al.* [41], ●. Predictions, ———. Predictions ($R = 0.56$), — — —.

buoyancy source (15) appearing in the transport equation for this correlation.

Both closure models for ε_t predict an integrated flux Richardson number, $-G_{kk}/P_{kk}$, of -0.25, whereas Ramaprian and Chandrasekhara [33] reported a measured value of about -0.15. Thus, in the calculations, the buoyancy contribution amounts to about 20% of the total production of the turbulent kinetic energy.

4.2.2. *Round plume.* For calculations with a variable time-scale ratio, the model predicts spreading rates of $d\delta_u/dx = 0.139$ and $d\delta_t/dx = 0.146$. The corresponding results for a constant value of R are very similar with $d\delta_u/dx = 0.143$ and $d\delta_t/dx = 0.15$. These values are substantially larger than the respective values of 0.112 and 0.104 measured by George *et al.* [40]. This discrepancy of about 25% in $d\delta_u/dx$ may be attributed to the round-jet spreading-rate anomaly referred to earlier, which is obviously carried over to the buoyancy-driven plume. However, the disagreement about $d\delta_t/dx$ seems not to arise solely from this quarter, because the model does not predict the correct relative behaviour of the velocity and temperature spreading. This discrepancy is also evident in the stress-transport predictions of Haroutunian and Launder [8], but not in the algebraic stress closure of

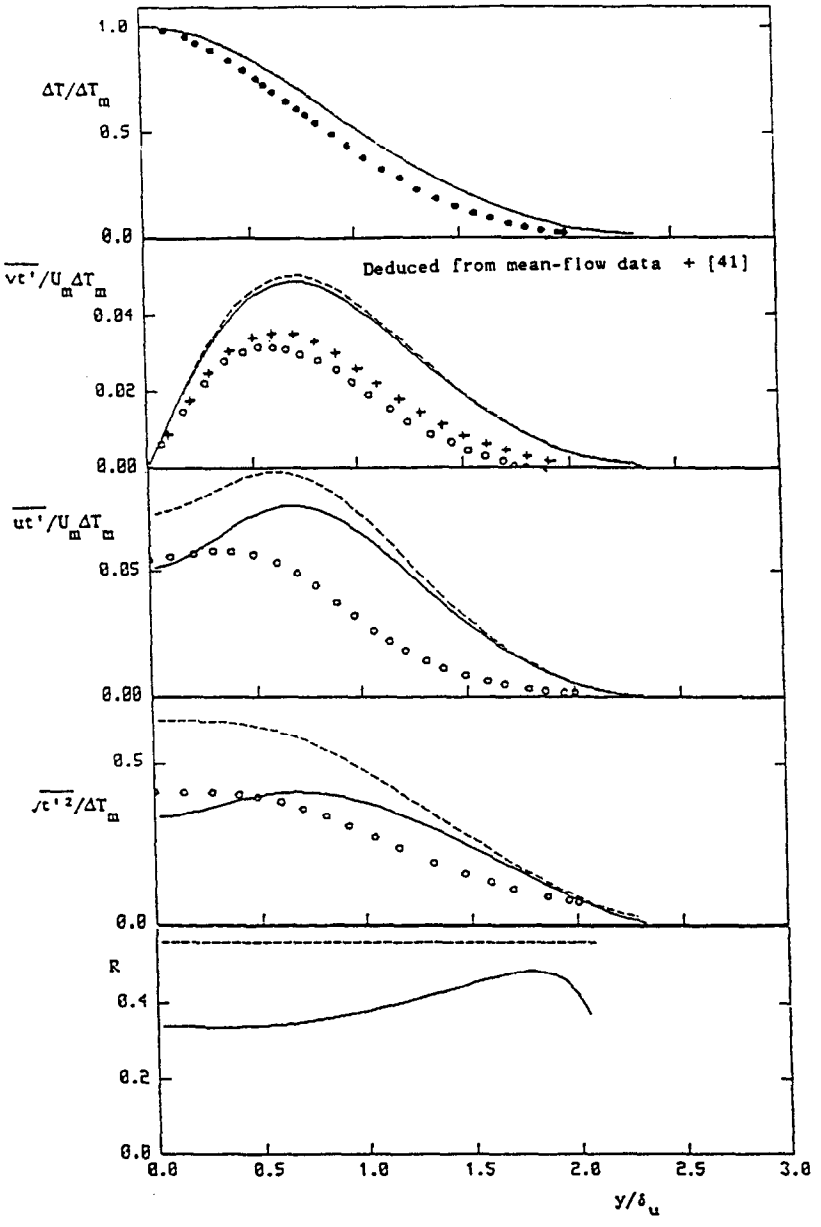

FIG. 8. Round free plume: similarity profiles of mean temperature, turbulent heat fluxes, temperature fluctuations and time-scale ratio. Data of: George *et al.* [40], ●; Beuther *et al.* [41], ○. Predictions, ———. Predictions ($R = 0.56$), — — —.

Hossain and Rodi [2]. This suggests that there is insufficient radial diffusive transport of $\overline{vt'}$ in the differential stress model, but it should also be noted that the algebraic closure has the advantage that it employs empirical corrections to predict correctly the radial transport of streamwise momentum.

For the present turbulence model, nearly equal spreading of the velocity and temperature fields ($d\delta_u/dx = 0.139$ and $d\delta_t/dx = 0.141$) can be obtained by increasing the coefficient c_t from 0.15 to 0.2, so as to enhance the radial diffusive transport of $\overline{vt'}$; this has the effect of decreasing $\overline{vt'}$, and hence the thermal spreading rate. While this practice leads to only marginal reductions in the thermal spreading rates (2% maximum) of the other test cases, it unfortunately results in a less satisfactory prediction of the shape of the $\overline{vt'}$ profile towards the edge of the round plume.

Figure 7 shows that the similarity profiles of the mean velocity are in very good agreement with the measurements [40]. The same figure reveals that the computed normal stress levels are in fairly good accord with the data [40, 41] close to the axis of the plume, but elsewhere the model tends to overpredict the turbulence levels. The computed shearing stresses are also too high, which is consistent with the overestimation of the plume spreading rate. The results

also show that the variation in R brought about by solving for ε_t, leads to a more marked reduction in turbulence levels than was found for the plane plume (see Fig. 5). However, the differences between the two sets of normal-stress predictions are not dramatic. It should be mentioned that the data on $\overline{w^2}$ were estimated by assuming $\overline{w^2} = \overline{v^2}$.

As may be seen from Fig. 8, the predicted temperature profile is somewhat wider than the measured one [40]. This defect is reflected in the overprediction of $d\delta_t/dx$ noted earlier, and is a consequence of the poor predictions of $\overline{vt'}$ due mainly to the overprediction of turbulence levels discussed above. Figure 8 also shows that the distributions of the mean temperature and radial heat flux are scarcely altered by the change in closure model for ε_t. However, it can be seen that the use of a variable time-scale ratio produces a large effect on the magnitudes of $\overline{t'^2}$ and $\overline{ut'}$, and the effect is much more pronounced than for the plane plume. The calculations with a constant time-scale ratio overpredict the level of temperature-fluctuation intensity by about 50%, whilst distinctly better levels of $\overline{t'^2}$ are found by solving the transport equation for ε_t. The improved predictions result from the strong reduction in R, which as may be seen in Fig. 8, decreases to an average value of about 0.34. The predictions of $\overline{ut'}$ are also improved because a fall in the temperature fluctuations causes a reduction in the generation rate of $\overline{ut'}$ by buoyancy forces.

Both sets of predictions indicate that 20% of the total vertical heat flux is borne by the turbulence. This contribution is 5% higher than the experimental value reported by George *et al.* [40], and indicates that a significant fraction of the total energy flux is provided by the high correlation between temperature and vertical velocity fluctuations. The integrated flux Richardson number is predicted at -0.44 which indicates that the buoyancy contribution amounts to about 30% of the total production rate of turbulent kinetic energy.

4.3. *Forced turbulent plumes*

In the foregoing sections, the limiting cases of jet and plume flows were predicted. In this section, the general situation of the forced plume is considered where there are present both initial momentum and buoyancy. Under certain conditions the flow may behave first like a pure jet and then show a gradual transition to behave like a pure plume in the far field [30]. For both plane and axisymmetric cases, calculations are performed for densimetric source Froude numbers of 1, 5, 50, 500 and 1000. In each case, the marching integration is carried out until the flow finally behaves like a pure plume. Uniform inlet conditions are chosen for each case so as to define the appropriate Froude number, $F_D = \rho_0 U_0^2/(gd\Delta\rho_0)$. Here $\Delta\rho_0$ is the density defect at the source, d the source dimension, and subscript 0 denotes a source condition.

The results are presented in terms of dimensionless plots of centre-line values of flow variables against vertical distance from the source. The data and predictions are plotted in Figs. 9 and 10 according to the scaling law of Chen and Rodi [30]. Figure 9 compares the predicted and experimental decay of the centre-line values of the velocity, density defect, vertical turbulent intensity, turbulent temperature intensity, and vertical turbulent heat flux. The corresponding results for axisymmetric forced plumes are given in Fig. 10. The experimental data in these figures are taken from the compilations of Chen and Rodi [30], Malin [3, 42] and Ogino *et al.* [43]. Both figures show the demarcation of the jet, transition and plume regions determined by Chen and Rodi [30] from their analysis of the experimental data. Calculations were made with both closure models for ε_t, but the plotted results were significantly different only for $\overline{t'^2}$ and $\overline{ut'}$. Therefore, both sets of predictions are shown only for these quantities, and for the remaining variables, results are given only for calculations made with a variable time-scale ratio.

4.3.1. *Decay of mean quantities.* For both planar and axisymmetric cases, Figs. 9 and 10 show that all the predictions eventually converge into a single curve beyond the zone of flow establishment. The calculations for $F_D = 1000$ cover the full range between pure jet and pure plume. A gradual change from jetlike to plumelike behaviour is observed, which agrees closely with the experimental data. Within the jet and plume regions respectively, similarity theory dictates that the centre-line velocity should decay as $x^{-(1+j)/2}$ and $x^{-j/3}$, and the density defect as $x^{-(1+j)/2}$ and $x^{-(2j+3)/3}$. For both plane and round cases, the predictions verify these similarity decay laws, and the calculated demarcation of the three regions of the forced plume are in agreement with experiment.

4.3.2. *Decay of turbulent quantities.* From the axial plots of dimensionless turbulent quantities given in Figs. 9 and 10, it can be seen that for both plane and axisymmetric geometries, the predictions obtained for each source Froude number all merge into a single curve when the flow becomes established. These figures also reveal that the predicted decay behaviour agrees with gradients representing the similarity decay laws for the plume regions. The agreement with experiment about the vertical velocity fluctuations is very good for planar cases, but not surprisingly the intensities are overpredicted for axisymmetric forced plumes. It may be recalled that the model overpredicts the intensity of the vertical fluctuations for the limiting case of the self-similar round plume. Figures 9 and 10 show that of the two sets of predictions for the centre-line values of $\overline{ut'}$ and $\overline{t'^2}$, the calculations with a constant time-scale ratio tend to produce the best agreement with experiment.

5. CONCLUSIONS

The present study has demonstrated that the main features of vertical plane and round turbulent jets and plumes are predicted with reasonable accuracy by a

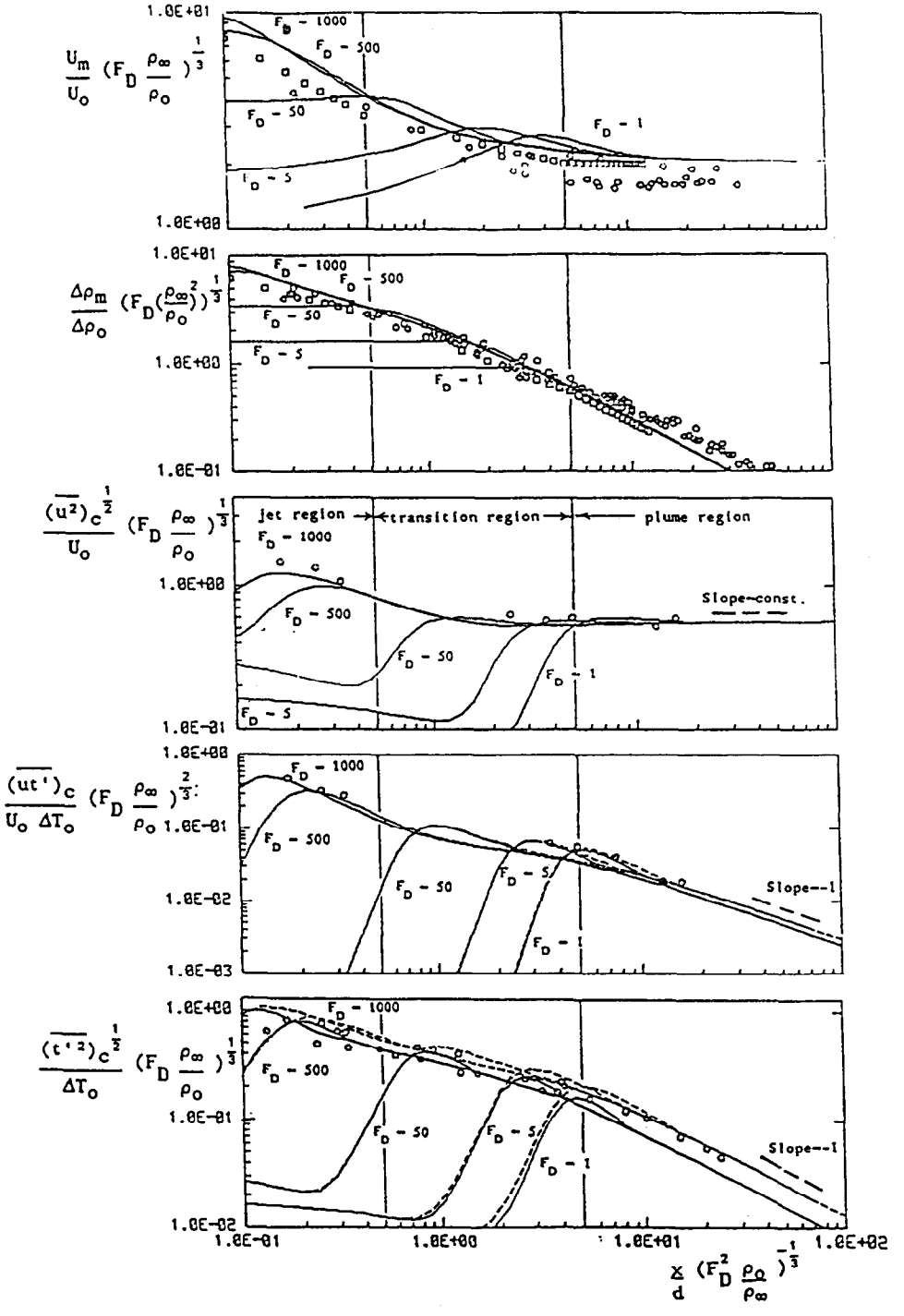

FIG. 9. Plane forced plume: experimental and predicted decay of centre-line mean and turbulent quantities. Symbols are data taken from Malin [42] and Chen and Rodi [30]. Predictions, ———. Predictions ($R = 0.56$), — — —.

revised Reynolds stress and heat flux transport closure. The main findings of the work are listed below.

(a) Solutions to the self-similar round jet show substantially better predictions than achieved with the old set of model coefficients proposed by Gibson and Launder [7], although the velocity spreading rate is still about 20% greater than experiment. The plane jet case is predicted fairly well by the model.

(b) Calculations of plane plumes with $c_{3\varepsilon} = c_{1\varepsilon}$ display rates of spread that are 20% lower than exper-

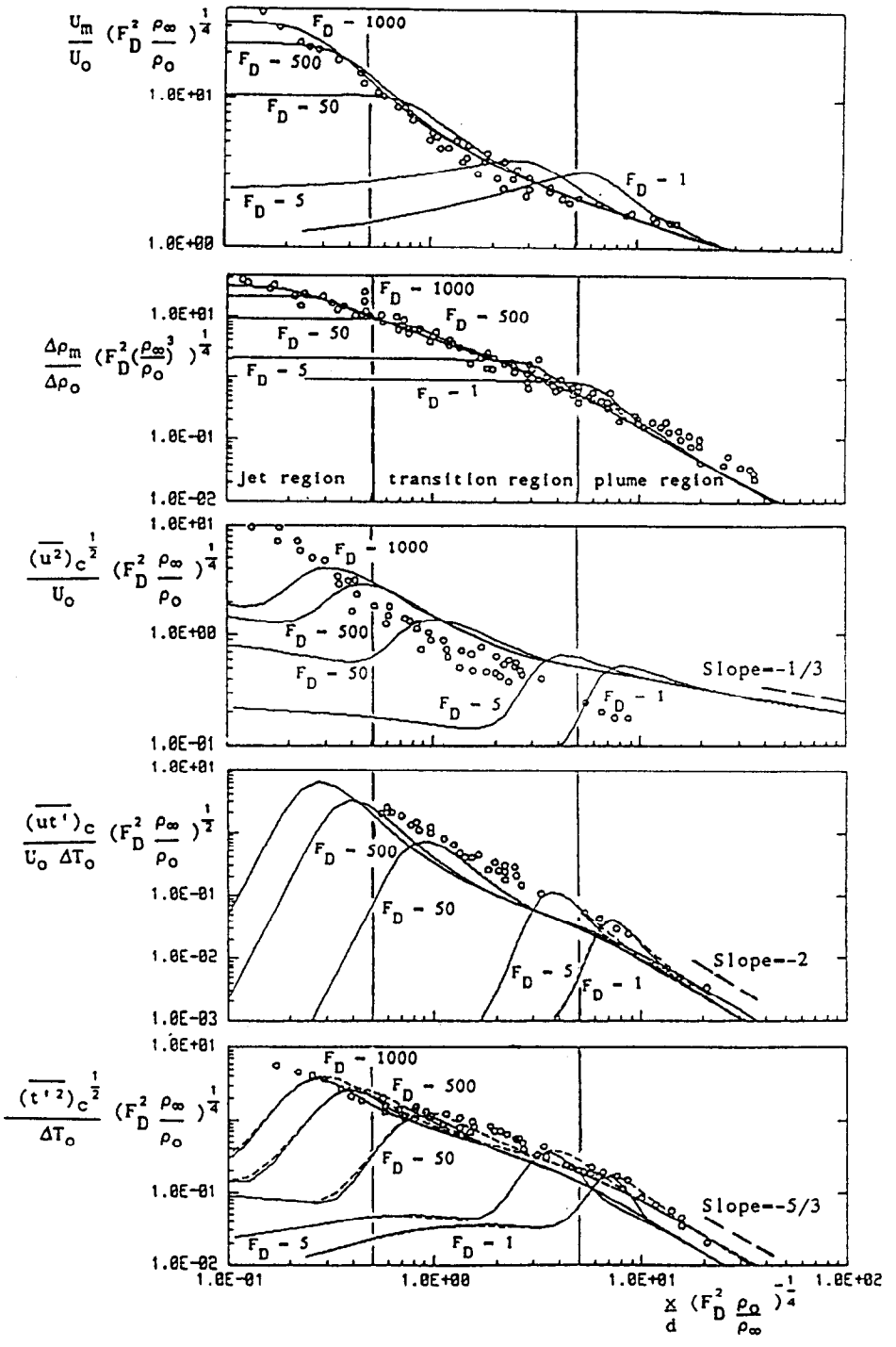

FIG. 10. Round forced plume: experimental and predicted decay of centre-line mean and turbulent quantities. Symbols are data taken from Malin [42], Chen and Rodi [30] and Ogino *et al.* [43]. Predictions, ———. Predictions ($R = 0.56$), — — —.

iment, but good agreement with the measured behaviour can be obtained by reducing the model coefficient $c_{3\varepsilon}$ to 70% of its original value.

(c) The predictions of axisymmeric plumes are less satisfactory than the plane cases, mainly because of the shortcomings associated with the failure of the model to predict correctly the growth rate of the axisymmetric jet.

(d) For jet flows, the modelled transport equation for ε_t predicts broadly the correct levels of fluctuating temperature, but the predictions are no better than those obtained with a constant time-scale ratio. The

transport model also predicts correctly that the time-scale ratio decreases under the influence of buoyancy, and this feature leads to improved predictions of $\overline{t'^2}$ for the round plume. However, the model underestimates the level of temperature fluctuations for plane plumes, and better results are obtained with a constant time-scale ratio.

(e) The Reynolds stress and heat flux transport model is capable of reproducing with reasonable accuracy the main features of turbulent forced plumes, where the flow undergoes a gradual transition from jetlike to plumelike behaviour.

The work presented in this paper forms part of an ongoing program of research concerned with the development of a Reynolds-stress/flux turbulence closure model for predicting practical buoyancy flows. In future work, attention will be focused on applying the model to both bounded and stratified buoyant flows. It is intended that further refinement to the model should concentrate on the closure approximations employed for the heat-flux and dissipation-rate equations.

REFERENCES

1. F. Tamanini, The effect of buoyancy on the turbulent structure of vertical round jets, *ASME J. Heat Transfer* **100**, 659–664 (1978).
2. M. Hossain and W. Rodi, A mathematical model for buoyant flows and its application to vertical buoyant jets. In *Turbulent Buoyant Jets and Plumes*, pp. 121–178. Pergamon Press, Oxford (1982).
3. M. R. Malin, Turbulence modelling for flow and heat transfer in jets, wakes and plumes, Ph.D. Thesis, University of London (1986).
4. J. J. McGuirk and C. Papadimitriou, Buoyant surface layers under fully entraining and internal hydraulic jump conditions, *Proc. 5th Symp. Turbulent Shear Flows*, Cornell University (1985).
5. B. E. Launder, G. J. Reece and W. Rodi, Progress in the development of a Reynolds-stress turbulence closure, *J. Fluid Mech.* **68**(3), 537–566 (1975).
6. B. E. Launder, On the effect of a gravitational field on the turbulent transport of heat and momentum, *J. Fluid Mech.* **67**, 569–581 (1975).
7. M. M. Gibson and B. E. Launder, Ground effects on pressure fluctuations in the atmospheric boundary layer, *J. Fluid Mech.* **86**, 491–511 (1978).
8. M. Haroutunian and B. E. Launder, Second-moment modelling of free buoyant shear flows: a comparison of parabolic and elliptic solutions, IMA Conf. on Stably Stratified Flow and Dense Gas Dispersion, Chester, pp. 409–430 (1986).
9. M. R. Malin and B. A. Younis, Modelling Reynolds stress and heat flux transport in turbulent buoyant plumes, *Proc. XXIII IAHR Congress on 'Hydraulics and the Environment'*, Ottawa, Canada, 21–25 August 1989, D9–D16 (1989).
10. M. M. Gibson and B. A. Younis, Modelling the curved turbulent wall jet, *AIAA J.* **20**(12), 1707–1712 (1982).
11. M. M. Gibson and B. A. Younis, Calculation of swirling jets with a Reynolds stress closure, *Physics Fluids* **29**, 38–48 (1986).
12. M. M. Gibson and B. A. Younis, Calculation of boundary layers with sudden transverse strain, *ASME J. Fluids Engng* **108**, 470–475 (1986).
13. B. A. Younis, On modelling the effects of streamline curvature on turbulent shear flows, Ph.D. Thesis, University of London (1984).
14. M. R. Malin and B. A. Younis, Reynolds-stress modelling of the turbulent wall jet in stagnant surroundings, *AIAA J.* (1990), in press.
15. W. P. Jones and P. Musonge, Modelling of scalar transport in homogeneous turbulent flows, *Proc. 4th Symp. Turbulent Shear Flows*, Karlsruhe University, 17.18 (1983).
16. W. P. Jones and P. Musonge, Closure of the Reynolds stress and scalar flux equations, *Physics Fluids* **31**(12), 3589–3604 (1988).
17. O. Zeman and J. L. Lumley, Buoyancy effects in entraining turbulent boundary layers: a second order closure study. In *Turbulent Shear Flows I*. Springer, Heidelberg (1979).
18. B. J. Daly and F. H. Harlow, Transport equations of turbulence, *Physics Fluids* **13**, 2634–2649 (1970).
19. J. C. Rotta, Statistische theorie nichthomogener turbulenz, *Z. Phys.* **129**, 547–572; **131**, 51–77 (1951).
20. A. S. Monin, On symmetry properties of turbulence in the surface layer of air, *Izv. Akad. Nauk., SSSR, Fizika Atmosf.* 11 (1965).
21. K. S. Liauw, Turbulent buoyant jets and plumes, M.Phil. Thesis, Faculty of Engineering, University of London (1984).
22. D. B. Spalding, Concentration fluctuations in a round turbulent free jet, *Chem. Engng Sci.* **26**, 95–167 (1971).
23. B. E. Launder, Heat and mass transport. In *Topics in Applied Physics 12*, Chap. 6. Springer, Berlin (1976).
24. G. R. Newman, B. E. Launder and J. L. Lumley, Modelling the behaviour of homogeneous scalar turbulence, *J. Fluid Mech.* **111**, 217 (1981).
25. S. Elghobashi and B. E. Launder, Modelling the dissipation rate of temperature variance in a thermal boundary layer, *Proc. 3rd Symp. Turbulent Shear Flows*, University of California, Davis, 15.13 (1981).
26. H. I. Rosten and D. B. Spalding, The PHOENICS beginner's guide, CHAM TR/100, CHAM Ltd, London (1985).
27. L. J. S. Bradbury, The structure of a self-preserving turbulent jet, *J. Fluid Mech.* **23**, 31–64 (1965).
28. E. Gutmark and I. Wygnanski, The planar turbulent jet, *J. Fluid Mech.* **73**, 465–495 (1976).
29. W. Rodi, The prediction of free turbulent boundary layers by use of a two-equation model of turbulence, Ph.D. Thesis, University of London (1972).
30. C. J. Chen and W. Rodi, *Vertical Turbulent Buoyant Jets—A Review of Experimental Data*. Pergamon Press, Oxford (1980).
31. F. C. Gouldin, R. W. Schefer, S. C. Johnson and W. Kollmann, Nonreacting turbulent mixing flows, *Proc. Energy Combust. Sci.* **12**, 257–303 (1986).
32. B. G. Van der Hegge Zijnen, Measurement of the velocity distribution in a plane turbulent jet of air; Measurement of the distribution of heat and matter in a plane turbulent jet of air, *Appl. Scient. Res.* **A7**, 256–292 (1958).
33. B. R. Ramaprian and M. S. Chandrasekhara, Study of vertical plane turbulent jets and plumes, IIHR 257, University of Iowa (1983).
34. J. Bashir and M. S. Uberoi, Experiments on turbulent structure and heat transfer in a two-dimensional jet, *Physics Fluids* **18**, 405–410 (1975).
35. E. J. List, Mechanics of turbulent buoyant jets and plumes. In *Turbulent Buoyant Jets and Plumes*, pp. 1–68. Pergamon Press, Oxford (1982).
36. R. A. Antonia, On a heat transport model for a turbulent plane jet, *Int. J. Heat Mass Transfer* **10**, 1805–1812 (1985).
37. R. Chevray and N. K. Tutu, Intermittency and preferential transport of heat in a round jet, *J. Fluid Mech.* **88**(1), 133–160 (1978).

38. R. A. Antonia, A. Prabhu and S. E. Stephenson, Conditionally sampled measurements in a heated turbulent jet, *J. Fluid Mech.* **72**(3), 455–480 (1975).
39. H. A. Becker, H. C. Hottel and G. C. Williams, The nozzle-fluid concentration field of the round turbulent free jet, *J. Fluid Mech.* **30**, 285–303 (1967).
40. W. K. George, R. L. Alpert and F. Taminini, Turbulence measurements in an axisymmetric buoyant plume, *Int. J. Heat Mass Transfer* **20**, 1145–1154 (1977).
41. P. D. Beuther, S. P. Capp and W. K. George, Momentum and temperature balance measurements in an axisymmetric turbulent plume, ASME Publication 79-HT-42 (1979).
42. M. R. Malin, The decay of mean and turbulent quantities in vertical forced plumes, *Appl. Math. Modelling* **11**, 301–314 (1987).
43. F. Ogino, H. Takeuchi, M. Ohki and T. Mizushina, Turbulence measurements in an axisymmetric buoyant jet, *Proc. 3rd Symp. on Turbulent Shear Flows*, Davis, California (1981).

CALCUL DES PANACHES TURBULENTS AVEC FERMETURE PAR LES TENSIONS DE REYNOLDS ET LES FLUX DE CHALEUR

Résumé—On adopte une fermeture différentielle des tensions de Reynolds et des flux de chaleur pour modéliser la convection de chaleur et de quantité de mouvement dans des panaches libres verticaux. Les équations sont résolues pour les tensions et les flux thermiques, la dissipation de l'énergie turbulente et les moyennes quadratiques des fluctuations de température. La fermeture permet de traiter les mécanismes de transport turbulent de façon plus exacte que par les modèles à deux équations de type Boussinesq qui sont basés sur la notion d'une viscosité et d'une diffusivité effective. Le modèle est appliqué au calcul des panaches self-similaires et des panaches forcés. Les résultats sont comparés aux données expérimentales et ils sont en accord raisonnable avec les observations.

BERECHNUNG TURBULENTER AUFTRIEBSFAHNEN

Zusammenfassung—Der turbulente Energie- und Impulstransport in senkrechten freien Auftriebsfahnen wird mit Hilfe einer differentiellen Schließbedingung für Reynolds'sche Schubspannung und Wärmestrom modelliert. Die Transportgleichungen werden für turbulente Schubspannungen und Wärmeströme, die Dissipationsrate der Turbulenzenergie und die mittleren quadratischen Temperaturschwankungen gelöst. Eine Schließbedingung an dieser Stelle erlaubt eine exaktere Berechnung der turbulenten Transportvorgänge als bei Zwei-Gleichungs-Modellen nach Boussinesq, welche auf der Einführung von Effektivwerten für Viskosität und Diffusivität beruhen. Außerdem wird die Lösung einer Transportgleichung für die thermische Dissipation untersucht, welche ohne eine empirische Beschreibung des Verhältnisses der thermischen und mechanischen Zeitmaßstäbe auskommt. Das Modell wird für die Berechnung von selbstähnlichen Auftriebsfahnen und erzwungenen Auftriebsfahnen angewandt. Die Ergebnisse werden mit vorhandenen Versuchsdaten verglichen, wobei sich eine brauchbare Übereinstimmung ergibt.

РАСЧЕТ ТУРБУЛЕНТНЫХ ВОСХОДЯЩИХ СВОБОДНОКОНВЕКТИВНЫХ ТЕЧЕНИЙ С ЗАМЫКАНИЕМ УРАВНЕНИЙ ПУТЕМ УЧЕТА РЕЙНОЛЬДСОВСКИХ НАПРЯЖЕНИЙ И ПЕРЕНОСА ТЕПЛОВОГО ПОТОКА

Аннотация—Замыкание с помощью дифференциальных рейнольдсовских напряжений и тепловых потоков используется при моделировании турбулентного переноса тепла и импульса в вертикальных свободноконвективных факелах. Полученные уравнения переноса решаются для турбулентных напряжений и тепловых потоков, скорости диссипации энергии турбулентности и среднеквадратичных пульсаций температуры. Используемая процедура замыкания позволяет более точно исследовать процессы турбулентного переноса, чем двухпараметрические модели типа Буссинеска, основанные на понятии эффективной вязкости и температуропроводности. Также проведен анализ решения уравнения переноса для диссипации энергии, в котором не требуется задавать эмпирически отношение временных масштабов тепловых и механических процессов. Предложенная модель применяется для расчета как самосогласованных, так и вынужденных восходящих факелов. Полученные результаты сравниваются с имеющимися экспериментальными данными, и найдено, что они удовлетворительно согласуются с результатами измерений.